Available online at www.sciencedirect.com

SciVerse ScienceDirect

Ceramics International 39 (2013) 2519–2526

CERAMICS INTERNATIONAL

www.elsevier.com/locate/ceramint

Synthesis, processing and characterization of a bioactive glass composition for bone regeneration

Dilshat U. Tulyaganov[a,b,*], Mokhir E. Makhkamov[c], Alisher Urazbaev[c], Ashutosh Goel[d], José M.F. Ferreira[a]

[a]*Department of Materials Engineering and Ceramics, University of Aveiro, CICECO, 3810-193 Aveiro, Portugal*
[b]*Turin Polytechnic University in Tashkent, 100095 Tashkent, Uzbekistan*
[c]*Tashkent Medical Academy, 100000, Tashkent, Uzbekistan*
[d]*Sterlite Technologies Ltd., E1, E2, E3, MIDC Waluj, Aurangabad 431136, India*

Received 3 July 2012; received in revised form 4 September 2012; accepted 4 September 2012
Available online 12 September 2012

Abstract

This paper reports on the experimental evaluation of a novel melt-quenched glass belonging to the $CaO–MgO–SiO_2–P_2O_5–Na_2O–CaF_2$ system as potential material for biomedical applications in bone regeneration. The glass composition has been designed in the primary crystallisation field of pseudo-wollastonite in $CaO–MgO–SiO_2$ ternary phase diagram. The rise of pH upon immersion in SBF solution was slower for the novel glass in comparison to 45S5 Bioglass®. Nevertheless, both glasses exhibited similar behaviour in early formation of crystalline apatite demonstrating their osteoinductive features. The *in vivo* investigations in rabbits demonstrated good compatibility between the glass and surrounding tissue along the whole implantation period with negligible adverse reactions. The clinical evaluation of glass has been conducted in accordance with the ethical guidelines and regulations.

Keywords: Synthesis; Bioglasses; SBF; Biodegradation

1. Introduction

Defects in bone structure arise in a variety of circumstances, such as casualties, surgery, diseases, etc. creating a need for skeletal reconstruction [1]. An ideal biomaterial is expected to be bioactive and exhibit optimum degradation rate so as to support the replacement of normal tissue without inflammation. A variety of bone substitutes is available and numerous efforts have been made to reconstruct the normal function of the skeletal system. However, the outcome of such efforts still has many limitations and problems [2–4]. Various bioactive and biocompatible glasses have been developed as bone replacement materials owing to their ability to resorb via a combination of cellular mechanism and chemical dissolution leading to bone regeneration and to control gene transcription through glass dissolution products [5–7]. However, still the 45S5 Bioglass® discovered by Hench et al. [5,8,9] is still taken as a standard for most of the designed bioactive glass compositions. It is nowadays used successfully as middle ear and dental implants but, as reported elsewhere [10–12], it has the potential to be used in many more bioactive applications than hydroxyapatite.

In the last few years, our research group has been dealing with the design and development of bioactive glasses in the $CaO–MgO–SiO_2$ system for their potential applications in human biomedicine [13–17]. The glass compositions were selected in the primary crystallisation field of pseudo-wollasotine phase in the ternary $CaO–MgO–SiO_2$ diagram doped with P_2O_5, Na_2O, CaF_2 and B_2O_3 in order to obtain glasses with their silicate glass network being dominated by Q^2 (Si) species [18–20]. For phospho-silicate glasses it has been reported that the highest level of bioactivity can be expected when Q^n (Si) units (n: number of bridging oxygens) are dominated by chains of Q^2 metasilicates, which are occasionally cross-linked

*Corresponding author at: Turin Polytechnic University in Tashkent, 100095 Tashkent, Uzbekistan.
E-mail address: ddilshod@bcc.com.uz (D.U. Tulyaganov).

0272-8842/$ - see front matter © 2012 Published by Elsevier Ltd and Techna Group S.r.l.
http://dx.doi.org/10.1016/j.ceramint.2012.09.011

through Q^3 units, whereas Q^1 units terminate the chains [21]. The investigated glass compositions exhibited high rates of bioactivity *in vitro*, i.e., upon immersion in simulated body fluid and of osteoblast proliferation in cell culture medium, and no evidence of any toxicity or other detrimental effects in the functionality of cells, which qualifies them for their further experimentation *in vivo* [15].

The present study aims at deeply investigating *in vitro* bioactivity of novel bioactive glass, its biodegradation behaviour as well as to discuss the results of the animal tests and data received from some preliminary clinical trials.

2. Materials and methods

2.1. Glass composition design and glass synthesis

In the light of the above mentioned perspective, a glass has been designed in the primary field crystallisation field of pseudo-wollastonite in the $CaO–MgO–SiO_2$ with nominal composition: (wt%) 4.53 Na_2O, 28.66 CaO, 8.83 MgO, 46.06 SiO_2, 6.22 P_2O_5, and 5.70 CaF_2. The designed glass composition is close to the composition of the liquid in the invariant equilibrium of the transition type (wt%) 51.4 SiO_2, 36.8 CaO, and 11.8 MgO, Eq. (1) [22]:

$$\text{Liquid} + \text{pseudowollastonite} \leftrightarrows \text{akermanite} + \text{wollastonite} \quad (1)$$

and the eutectic type (wt%) 51.6 SiO_2, 35.6 CaO, and 12.8 MgO [22], Eq. (2):

$$\text{Liquid} \leftrightarrows \text{wollastonite} + \text{diopside} + \text{akermanite} \quad (2)$$

The novel bioactive glass was produced in frit form by the melt-quenching technique as has been described in our previous study [15]. In parallel, the 45S5 Bioglass® was also prepared to act as the benchmark for comparing their degradation rates and *in vitro* bio-mineralisation performances. The glass frits were dried and then milled in a high-speed mill to obtain fine powders with mean particle sizes of about 10–15 μm (as determined by the light scattering technique; Coulter LS 230, UK, Fraunhofer optical model) and specific surface areas ranging between 0.3 and 0.7 $m^2\,g^{-1}$ (BET technique; Micromeritics, Gemini II 2370, USA).

2.2. In vitro biodegradation tests

The *in vitro* bioactivity of the glasses, reflected in their capability of inducing hydroxyapatite (here after referred as HA) formation onto their surfaces, was investigated by immersing the glass powders in SBF (0.1 g glass powder in 50 ml SBF solution) at 37 °C. SBF had an ionic concentration (Na^+ 142.0, K^+ 5.0, Ca^{2+} 2.5, Mg^{2+} 1.5, Cl^- 125.0, HPO_4^- 1.0, HCO_3^{2-} 27.0, and SO_4^{2-} 0.5 $mmol\,l^{-1}$) nearly equivalent to human plasma, as discussed by Tas [23]. The powder–SBF mixtures were immediately sealed into sterilised plastic flasks and stored in an oven at 37 ± 0.5 °C. After each experiment, the powders were separated from the liquids by filtering. Sampling took place at different times between 1 h and 21 days. The obtained results were independent, which means that each sample was individually treated without interfering with others. The experiments were made in triplicate in order to assure the reproducibility of the results obtained.

The degradation tests were performed according to the standard ISO 10993-14 "Biological evaluation of medical devices — Part 14: identification and quantification of degradation products from ceramics". The test aims at studying the degradation behaviour of glasses/ceramics in the most frequently encountered *in vivo* pH (7.4 ± 0.1) and, therefore, investigates the degradation of glasses/ceramics in freshly prepared Tris–HCl buffered solution. The tests were carried out without solution replacement at 37 °C and with a mixing speed of 120 rpm. The sampling was done after duration of 120 h where the solid and liquid phases were separated by filtering (0.22 μm, Millex GP, Millipore Corporation, USA). The solid samples were then washed in deionised water and dried in an oven to constant weight. A relative weight loss percentage (W_L) of glass samples after 120 h of immersion in solutions was calculated from the following equation:

$$W_L = \left(\frac{W_0 - W_t}{W_0}\right) \times 100,$$

where W_0 refers to the weight of glasses before immersion and W_t refers to the weight of glasses after immersion.

The analysis of the liquids comprised of pH measurements (CONSORT P800, Belgium). The glass powders separated from the liquids were subjected to X-ray diffraction (XRD; $2\theta = 20°–50°$ with a 2θ-step of 0.02 deg s^{-1}; Rigaku Geigerflex D/Mac, C Series, Cu K_α radiation, Japan) and infrared spectroscopy analysis (FTIR, model Mattson Galaxy S-7000, USA). In order to obtain infrared spectra, glass powders were mixed with KBr in the proportion of 1/150 (by weight) and pressed into a pellet using a hand press. 64 scans for background and 64 scans per sample were made with signal gain 1. The resolution was 4 cm^{-1}.

2.3. In vivo tests

In vivo biocompatibility tests were conducted with bulk glasses and glass particulates of the investigated glass composition. The implantation and histological analyses of the bones with the implants were performed at the Division of Surgical Stomatology, Tashkent Medical Academy, Uzbekistan.

Healthy and completely matured (1-year old) rabbits from the breed "shinshilla" weighing 2.8–3.0 kg were used. Animals were kept in individual cages, properly identified according to the period and group. After applying systemic anaesthesia, non-polished rectangular prisms (ca. $2 \times 2 \times 10$ mm^3), previously sterilised in alcohol and boiled in distilled water, were implanted in the femoral diaphysis

region in a drilled hole of 2 mm diameter and about 10 mm length. Similar holes were also filled with 0.1 g of the respective glass particles, sterilised in dry heat at 180 °C for 2 h prior to implantation. The incised hole was subsequently sewed up. Incision without any implantation was also performed as control. The reactions of the animals were monitored during the implantation periods: 1 week; 2 weeks; 1 month; 2 months; 3 months; 4 months and 6 months. After implantation, the rabbits were sacrificed by immediate decapitation. The surgeries and animal care were undertaken in accordance with ethical guidelines and rules of local Governmental bodies. All femurs were subsequently fixed in 10% phosphate buffered formalin for 72 h for histology or histomorphometry analysis. These femurs were decalcified in 10% formic acid formalin solution for 14 days. The femurs were sectioned parallel to the long axis of the femur through the anteromedial aspect of the defect. The tissue blocks were sectioned and stained with hematoxilin and eosin (H&E) and histopathologically observed by optical microscopy. During the implantation period the rabbits exhibited ordinary behaviour and no evidence of adverse reactions could be observed.

2.4. Design of the clinical trials

The permission for performing limited clinical tests was granted by the Pharmacological Committee of the Ministry of Health of Uzbekistan under reference no. 23, dated 26.11.2007, and the National Ethical Committee of Uzbekistan under reference no. 2, dated 5.02.2008. The protocol (programme) of clinical tests was then approved by the Chief of the Department of New Medical Techniques on 13.02.2008, thus allowing performance of limited clinical trials in the following two clinics: (a) Tashkent Medical Academy in the Clinic Hospital of the Urgent Medical Aid and (b) Tashkent Doctor's Qualification Upgrading Institute in the Town Clinic number 7.

Over a period of 8 months clinical tests were performed to the treat jaw bone defects left mainly after cystectomy operation on 45 patients including 21 males and 24 females with ages in the range of 19–60 years old. The clinical trials were conducted with prior consent of all patients who agreed to participate in this study on a voluntary basis. According to the protocol design, all the patients were clinically examined before (day 0), and after surgery (days 15th, 60th and 180th). Retro alveolar X-ray radiographs were always taken after each time period

Before cystectomy operation, a general clinical examination of patient including X-ray radiography was performed. It allowed estimation of the wound volume and the amount of bone graft to be applied. After cystectomy, the defect area and the dissected frontal wall of the jaw were carefully rinsed several times with 3% of hydrogen peroxide and 0.05% chlorhexadine solutions to wash out the cystic tissue completely. The required amount of sterilised glass particulates was mixed with the fresh blood from the defective region and then used to completely fill the bone defect. Finally, the surgical sites were closed by returning to the original position and fixed. The patients were recommended to use appropriate postoperative antibiotic whether it was prescribed, and to follow home care regime.

3. Results

3.1. In vitro bioactivity and leaching tests

Fig. 1 shows the pH variations as a function of the immersion time as a result of the solubility/ionic exchange reactions occurring at the solid/liquid interface. It can be seen that more noticeable changes have occurred in the earliest immersion period, especially in the case of 45S5 Bioglass®. This is not surprising considering that the sodium content of 45S5 Bioglass® is about 5 times more than that of the new bioglass. During the first 7 days (168 h) of immersion in SBF, the pH of the 45S5 Bioglass® increased from 7.10 (the initial pH of SBF solution) to 7.72, followed by gradual smaller increments with increase in immersion time. The pH rise was more sluggish in the novel glass and the overall deviations from the initial pH of SBF solution were therefore smaller. According to the mechanism proposed by Hench [24], the exchange of Na^+/H^+ ions is responsible for the increase in pH.

Fig. 2a shows the XRD spectra of the novel bioglass before and after immersing in SBF for different time periods, while Fig. 2b depicts the same kind of plots for the 45S5 Bioglass® tested under the same experimental conditions. The spectra of both glasses before immersion are characteristic of amorphous materials showing a broad hump in the region 28–35°. After 3 days of immersion the main peak of hydroxyapatite (HA) at $2\theta \sim 32°$ can be clearly observed in the XRD spectra of both bioglasses, being more evident in the case of the novel composition. With further prolonging the soaking period to 21 days, this

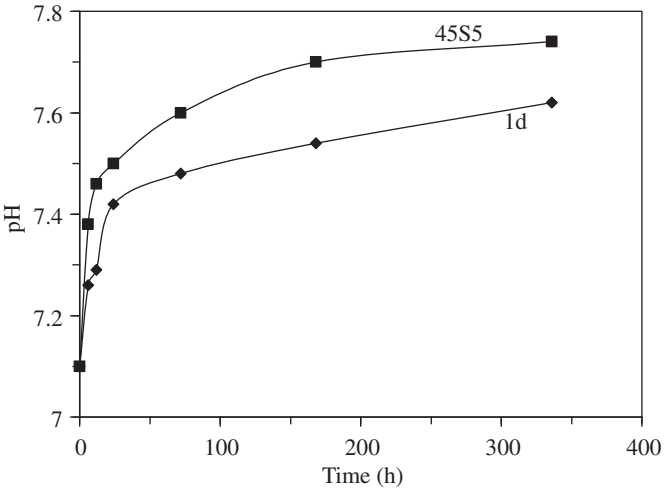

Fig. 1. Evolution of pH in SBF over 2 weeks of immersion in the glass powders: ■ – glass 1d; ♦ – 45S5 Bioglass®.

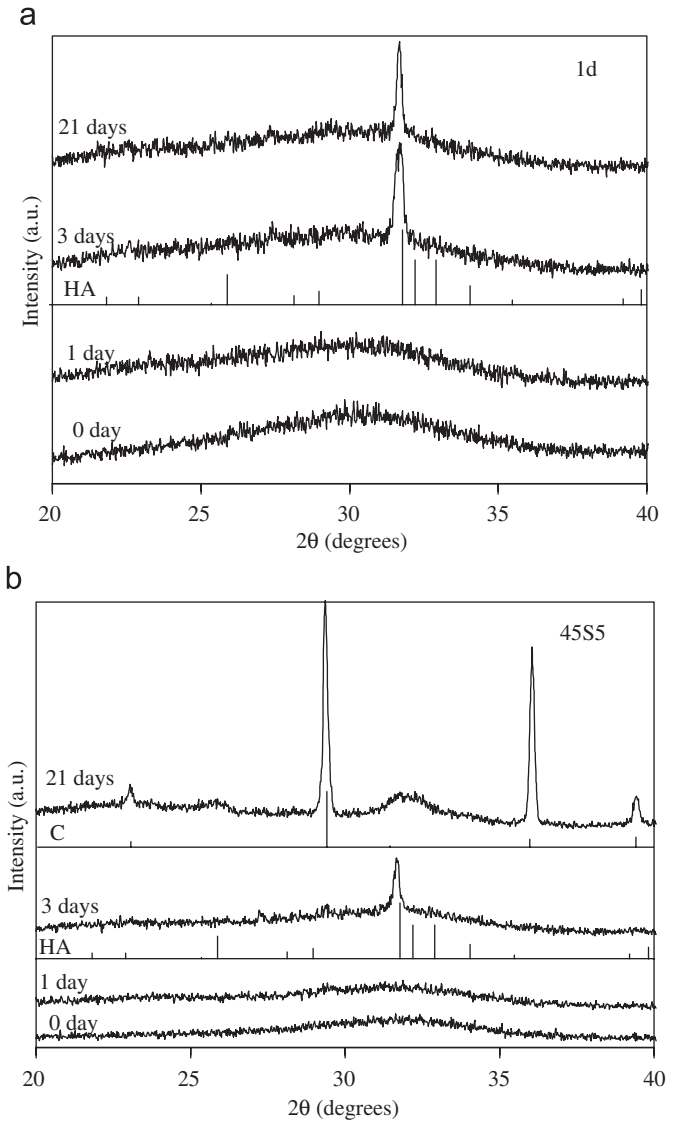

Fig. 2. XRD patterns of glass before and after immersion in SBF for several time periods: (a) glass 1d; and (b) 45S5 Bioglass®.

main HA peak became a bit sharper for the novel bioglass (Fig. 2a), while a decreased intensity was clearly noticed in the case of 45S5 Bioglass® (Fig. 2b). Moreover, in this last case, the observed decreasing intensity of HA peaks was accompanied by the formation of relatively high intensity calcium-carbonate (calcite) peaks, thus suggesting that the early deposited HA layer was gradually hidden by the freshly precipitated calcite. This precipitation sequence suggests an early depletion of P species in SBF solution due to the formation of HA and their slow leaching rate from the 45S5 Bioglass®. This depletion of P species can be understood considering that (i) the Ca/P ratio in the starting SBF solution (Ca/P=2.5) is higher than in the stoichiometric HA (Ca/P=1.67) and (ii) the homogeneous dissolution of 45S5 Bioglass® (Ca/P ≈ 4) would further enrich the liquid media in Ca species. When the solubility product of calcite (K_{sp} values ranging from 3.7×10^{-9} to 8.7×10^{-9} at 25 °C, depending upon the data source) [25] is exceeded, this phase starts precipitating. Accordingly, Fig. 2b shows that calcite was the major phase formed at the surface of 45S5 Bioglass® particles upon immersion in SBF solution for 21 days. Considering that the starting concentration of P species is the same for both systems, the precipitation of calcite in the case of 45S5 Bioglass®, together with the higher pH changes observed (Fig. 1) are strong evidences of its higher solubility/ionic exchange capability. These bio-mineralisation results are in good agreement with the different chemical degradation rates of the glasses in Tris–HCl, which revealed a considerably higher weight loss in case of 45S5 Bioglass® (3.7 wt%) in comparison to that of the novel bioglass (2.0 wt%). Also, the pH of Tris–HCl solution increased from the initial value of 7.2–9.7 after 21 days in the case of 45S5 Bioglass®, while the maximum pH value achieved for the novel bioglass was only 8.1.

Although under the present experimental conditions crystalline HA could not be detected for short immersion times, the first steps of the bio-mineralisation mechanism proposed by Hench [24] have likely occurred. Fig. 3 shows the FTIR spectra of the novel bioglass and of the 45S5 Bioglass®, before and after immersing in SBF for 1 day. As a matter of fact, considerable differences in the structure of glasses could be observed after 24 h of immersion in SBF in comparison to their parent glasses as depicted in Fig. 3. A strong low frequency band centred at470 cm^{-1}, ascribed to a deformation mode of silica layer that develops upon dissolving glass particles [11] could be seen in both the glasses after immersion in SBF solution

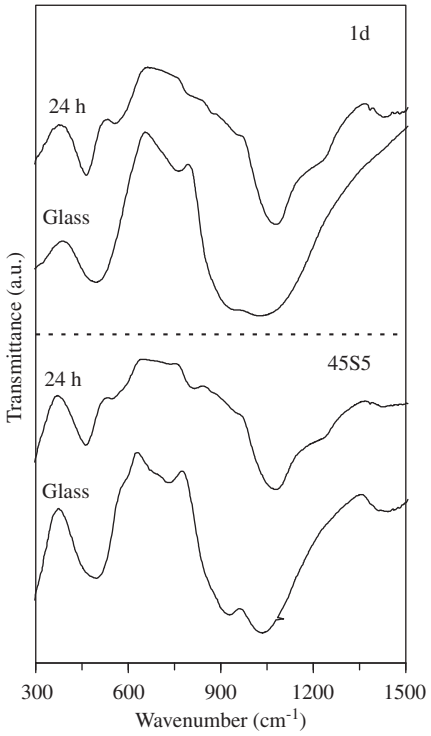

Fig. 3. FTIR spectra of the glasses 1d and 45S5 Bioglass® before and after immersing in SBF for 1 day.

for 1 day. The main IR band now occurs at 1090 cm^{-1} and a nearby shoulder, centred at ~1240 cm^{-1} and attributed to Si–O–Si vibration can be observed in both glasses due to the interfacial formation of high-area silica gel layer as postulated in Hench's inorganic reaction set [24].

3.2. In vivo animal tests

During the whole implantation period the rabbits exhibited ordinary behaviour without any evidence of adverse reactions. The items microscopically analysed included (i) the presence of inflammatory infiltrate (ii) the bone formation in the margins of the cavity (iii) the bone formation in the centre of the cavity and (iv) the presence of giant cells. Histopathological section of bone after 1 week of implantation showed low inflammatory infiltrate whereas an increase in the thickness of blood vessels was revealed (Fig. 4a). Abundant woven bone ingrowth and ongrowth and normal fibroblast proliferation were revealed after 2 weeks (Fig. 4b). In particular, new bone formation had originated from the margins of host bone towards the centre of cavities; the presence of single giant cells (macrophages) was also detected. Histology after 1 month demonstrated fragmentation of cavities by trabeculae, woven bone growth and initial stage of blood vessels formation. Moreover, mesenchymal stem cells (MSCs) at a weak differentiation stage could be observed at the periphery of cavities along with extensively developed collagen type structures of a connective tissue (Fig. 4c). The depth of bone ingrowths increased after 2 months and was accompanied with resorption of bone graft and formation of lamellar bone (Fig. 4d). By 3–4 months only residues of material completely embedded into bone trabeculae could be observed in newly formed bone tissue, i.e., new bone formation comprising osteoid type structures and remodelling occurred as evidenced by Fig. 4e and f. Finally, the cavities were completely filled with bone structures, and matured homogeneous bone tissue was formed after 6 months post-implantation period as can be seen in Fig. 4g.

3.3. The clinical trials

The glass particulates formed a cohesive mass with patient's blood demonstrating homoeostatic effect. The graft material was easy to place and shape *in situ*. The nearest results (from the first day to 90th day) demonstrated the absence of high degree of pain or signs of inflammation. No patient reported the occurrence of adverse clinical reactions or infectious complications in the postoperative phase. Usually patients are admitted on the day of surgery and discharged the next day. Complete clinical healing was considered when gums recuperated their natural colour, jaw could open and close easily and the teeth came together and separate easily. The patients' satisfaction was confirmed by their availability to undergo the procedures again if necessary. Furthermore, they would recommend the procedures to other patients.

It is worth mentioning that X-ray radiography was performed before the surgical operation. Examples of radiography images of a patient having radicular cyst in maxilla region are shown Fig. 5, before (Fig. 5a), and 2 months postoperative (Fig. 5b). It was revealed that 2 months postoperation the lesions were filled up with trabeculae of new bone. According to radiography data a radio-opaque line between bone graft and host bone was observed in the X-ray images after 2 months of implantation (Fig. 5b).

4. Discussion

Bioactive glasses have been used in medical applications for bone regenerative purposes as both monolithic structures and glass particulates [5,26]. Glass particulates with average particle sizes significantly smaller than 100 μm revealed to be very promising for a variety of applications in the field of regenerative medicine due to their antimicrobial and anti-inflammatory properties, as documented in some recent reports [27–28]. In the present study, mean particle size of the experimental glass powders was about 10–15 μm and both glasses exhibited formation of crystalline HA as early as after 3 days of soaking in SBF solution. It is known that reactivity, degradation and apatite formation in bioactive glasses are highly dependent on glass structure and network connectivity [21]. The numbers of non-bridging oxygens per each tetrahedral cation (NBO/T) was calculated for the novel glass and the 45S5 Bioglass® as 1.88 and 1.99, respectively, suggesting a more polymerised glass network structure for the investigated glass composition that contains predominantly Q^2, but features higher fraction of Q^3 units than 45S5 Bioglass® [19]. From the perspective of chemical composition, the novel glass contains similar amounts of SiO_2 and P_2O_5 as 45S5 Bioglass® and a bit higher amount of CaO. The significant differences in chemical compositions of two glasses can be summarised as follows and (i) the Na_2O content in the novel bioglass is about 5.4 times less; (ii) the novel bioglass also contains MgO and CaF_2, which are absent in the 45S5 Bioglass®. Magnesium is an element of high physiological interest in the biomedical field, being present in natural bony tissues and playing an essential role in human metabolism [29]. It is classified as an essential minor element and may have stimulatory effects on the growth of new bony tissues [30–31]. The introduction of Mg between 0.4 and 1.2 wt% in the bioactive glasses is known to improve the glass dissolution by disrupting the silica glass network [32] while it inhibits the crystallisation of apatite on the glass surface. On the other hand, partial substitution of CaF_2 for Na_2O in high alkali/alkaline-earth content phosphosilicate-based glasses is known to cause lower increment of pH [25], a feature that can be considered positive towards the proliferation of endothelial cells [33]. Generally, Na_2O–CaO–SiO_2–P_2O_5

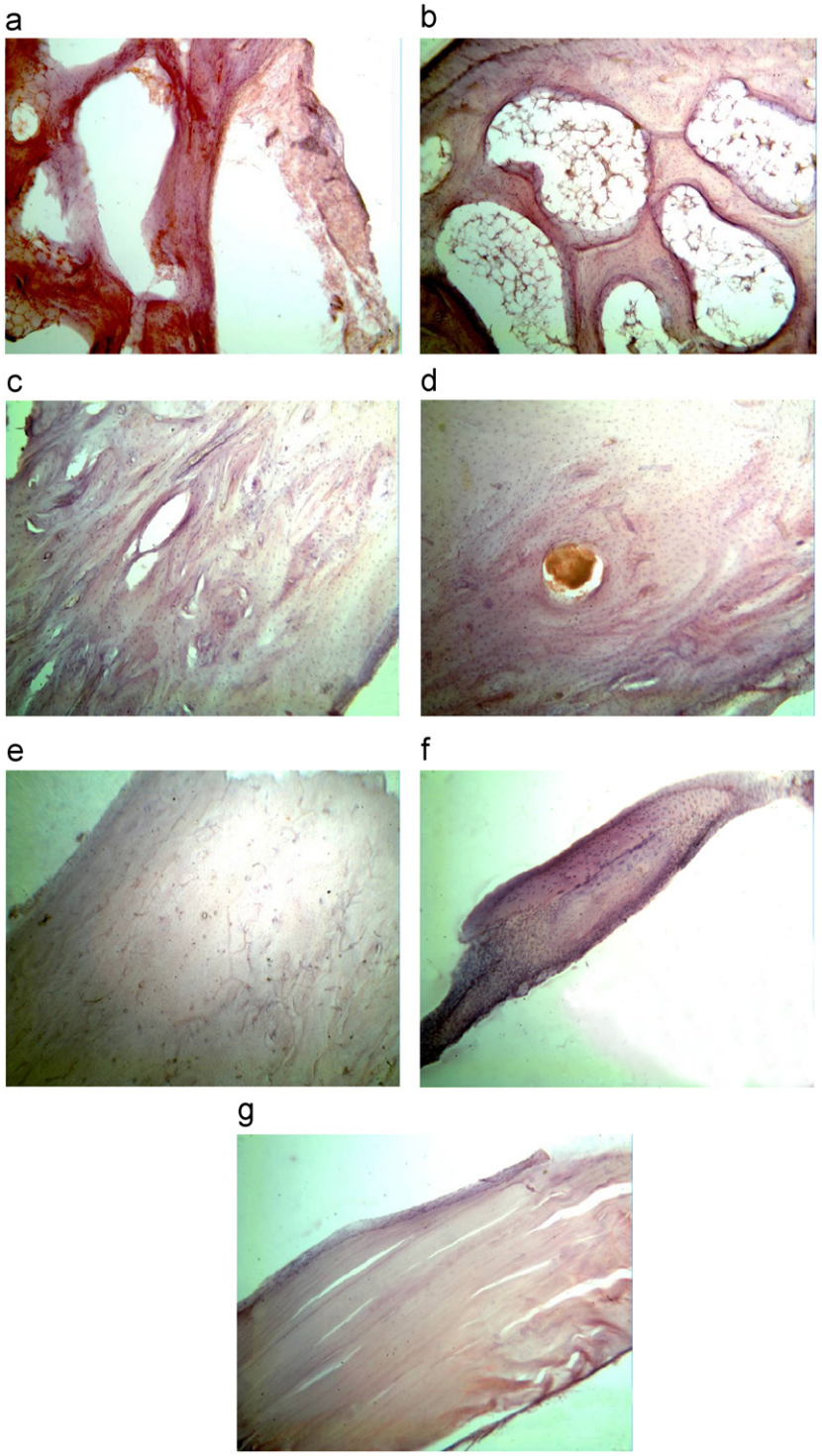

Fig. 4. Histopathological sections of the bone in cortical area of bone (HE X 400) after different periods of implantation: (a) 1 week; (b) 2 weeks; (c) 1 month; (d) 2 months; (e) 3 months; (f) 4 months; and (g) 6 months.

bioactive glasses are well known to cause a pH rise upon immersion in aqueous solutions which favours apatite deposition in SBF but can negatively affect the surrounding tissue *in vivo* [34]. The effect of fluoride content of the glass on the aqueous solution pH was explained by ion exchange processes occurring at the glass surface. Similar to Na^+ or Ca^{2+}, fluoride ions near the glass surface can go into solution, but in contrast to Na^+ or Ca^{2+} that are exchanged for H^+, fluoride can exchange for OH^- ions from the solution (from dissociation of water into H^+ and OH^-), which results in a pH decrease [34]. These favourable features explain the slower rise of pH upon immersion in SBF solution observed for the novel glass 1d compared to 45S5 Bioglass®. Nevertheless, both glasses exhibited

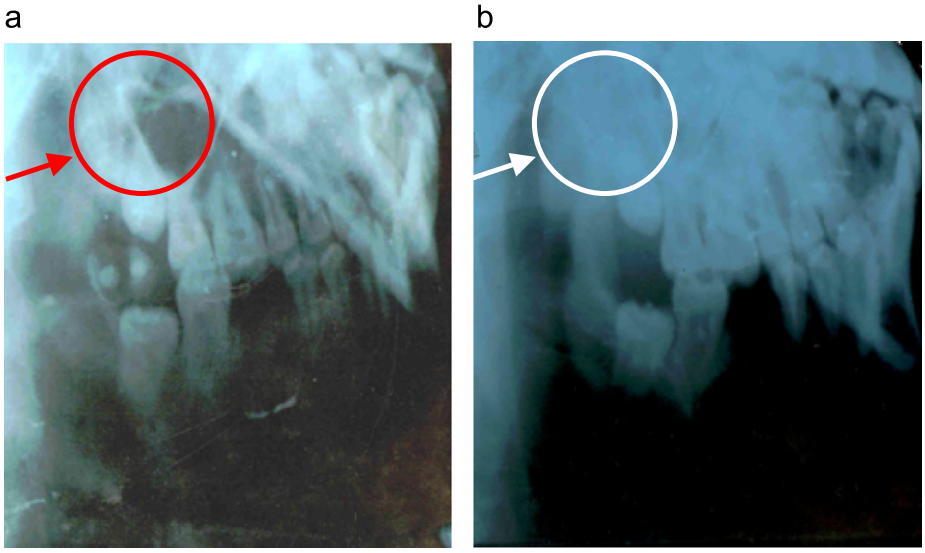

Fig. 5. Radiographs of the patient with radicular cyst lesion in maxilla region: (a) before operation and (b) 2 months postoperative.

similar behaviour in early formation of crystalline apatite (Figs. 2 and 3) demonstrating their osteoinductive features. The early formation of apatite can be understood considering that HA is the least soluble and most stable compound of calcium phosphate phases in aqueous solutions at pH values higher than 4.2 [23]. Calcite precipitation after prolonged soaking of 45S5 Bioglass® in SBF can be explained by its higher dissolution rate due to a less polymerised glass network. Thus, the higher pH rise for 45S5 Bioglass® caused greater quantities of cations such as Na^+ and in particular Ca^{2+} to be leached out that lead to calcite formation after the solution being depleted of P species [11].

The *in vivo* results obtained for the novel bioactive glass revealed that the material was fully compatible with the surrounding tissue along the whole implantation period without showing adverse reactions. The clinical tests in the treatment of cystic lesions demonstrated the safety and efficiency of the bioactive glass particulates in restoring the bone defects. Generally, cystic bone lesions are often self-healing or can even be cured by decompression [35]. Filling lesions with certain biomaterials leads to advanced bone generation because of the osteoconductive properties enhancing the migration of progenitor cells [36]. In this regard, experimental bioactive glass particulates can be used in the treatment of bone defects to remediate the progressive loss of the bone around teeth. Nevertheless, the results of long term clinical trials have to be obtained and a larger number of patients have to be treated before further considering the new glass particulates for medical practice.

5. Conclusions

A novel bioactive glass composition has been designed in the primary field crystallisation field of pseudo-wollastonite in the $CaO–MgO–SiO_2$. This glass demonstrated slower rise of pH upon immersion in SBF solution and slower chemical degradation rate in Tris–HCl compared to 45S5 Bioglass®. Although an apatitic layer was formed at the surface of both glasses in the early stage of immersion in SBF, the biomineralization behaviour differs under long *in vitro* experiments with calcite being preferentially deposited at the surface of 45S5 Bioglass®.

In the *in vivo* animal studies the novel material revealed low inflammatory infiltrate and was fully compatible with the surrounding tissue without showing any significant adverse reactions. In preliminary clinical trials the glass particulates demonstrated that this material would be particularly interesting in conventional treatment of bone defects. However, this assumption has to be confirmed by further experimentation over a longer period of time with a larger number of patients.

References

[1] N.K. Vail, L.D. Swain, W.C. Fox, T.B. Aufdlemorte, G. Lee, J.W. Barlow, Materials for biomedical applications, Materials and Design 20 (1999) 123–132.
[2] C. Merceron, C. Vinatier, J. Clouet, S. Colliec-Jouault, P. Weiss, J. Guicheux, Adipose-derived mesenchymal stem cells and biomaterials for cartilage tissue engineering, Joint Bone Spine 75 (6) (2008) 672–674.
[3] O.D. Schneider, F. Weber, T.J. Brunner, S. Loher, M. Ehrbar, P.R. Schmidlin, W.J. Stark, In vivo and in vitro evaluation of flexible, cottonwool-like nanocomposites as bone substitute material for complex defects, Acta Biomaterialia 5 (5) (2009) 1775–1784.
[4] P. Weiss, P. Layrolle, L.P. Clergeau, B. Enckel, P. Pilet, Y. Amouriq, G. Daculsi, B. Giumelli, The safety and efficacy of an injectable bone substitute in dental sockets demonstrated in a human clinical trial, Biomaterials 28 (22) (2007) 3295–3305.
[5] L.L. Hench, D.E. Day, W. Höland, V.M. Rheinberger, Glass and medicine, International Journal of Applied Glass Science 1 (1) (2010) 104–117.
[6] A. Hoppe, N.S. Güldal, A.R. Boccaccini, A review of the biological response to ionic dissolution products from bioactive glasses and glass-ceramics, Biomaterials 32 (11) (2011) 2757–2774.

[7] I.D. Xynos, A.J. Edgar, L.D.K. Buttery, L.L. Hench, J.M. Polak, Gene-expression profiling of human osteoblasts following treatment with the ionic products of bioglass 45S5 dissolution, Journal of Biomedical Materials Research 55 (2) (2001) 151–157.
[8] L.L. Hench, Bioactive Ceramics: Theory and Clinical Applications, Butterworth-Heinemann, Oxford, 1994.
[9] L.L. Hench, Glass and genes: the 2001 W. E. S. turner memorial lecture, Glass Technology 44 (1) (2003) 1–10.
[10] L. Lefebvre, J. Chevalier, L. Gremillard, R. Zenati, G. Thollet, D. Bernache-Assolant, Structural transformations of bioactive glass 45S5 with thermal treatments, Acta Materialia 55 (2007) 3305–3313.
[11] J. Schrooten, H.V. Oosterwyck, J.V. Vander Sloten, J.A. Helsen, Adhesion of new bioactive glass coating, Journal of Biomedical Materials Research 44 (1999) 243–252.
[12] L.L. Hench, Bioceramics—from concept to clinic, Journal of American Ceramic Society 74 (1991) 1487–1510.
[13] S. Agathopoulos, D.U. Tulyaganov, P. Valério, J.M.F. Ferreira, A new model formulation of the SiO_2–Al_2O_3–B_2O_3–MgO–CaO–Na_2O–F glass-ceramics, Biomaterials 26 (15) (2005) 2255–2264.
[14] S. Agathopoulos, D.U. Tulyaganov, J.M.G. Ventura, S. Kannan, M.A. Karakassides, J.M.F. Ferreira, Formation of hydroxyapatite onto glasses of the CaO–MgO–SiO_2 system with B_2O_3, Na_2O, CaF_2 and P_2O_5 additives, Biomaterials 27 (9) (2006) 1832–1840.
[15] D.U. Tulyaganov, S. Agathopoulos, P. Valerio, A. Balamurugan, A. Saranti, M.A. Karakassides, J.M.F. Ferreira, Synthesis, bioactivity and preliminary biocompatibility studies of glasses in the system CaO–MgO–SiO_2–Na_2O–P_2O5–CaF_2, Journal of Materials Science: Materials in Medicine 22 (2) (2011) 217–227.
[16] G.E. Stan, S. Pina, D.U. Tulyaganov, I. Pasuk, C.O. Morosanu, J.M.F. Ferreira, Highly adherent bio-glass sputtered films with bioactive properties, Journal of Materials Science: Materials in Medicine 21 (2010) 1047–1055.
[17] G.E. Stan, I. Pasuk, M.A. Husanu, I. Enculescu, S. Pina, A.F. Lemos, D.U. Tulyaganov, J.M.F. Ferreira, Highly adherent bioactive glass thin films synthetized by magnetron sputtering at low temperature, Journal of Materials Science: Materials in Medicine 22 (2011) 2693–2710.
[18] I. Kansal, D.U. Tulyaganov, A. Goel, M.J. Pascual, J.M.F. Ferreira, Structural analysis and thermal behaviour of diopside-fluorapatite–wollastonite-based glasses and glass-ceramics, Acta Biomaterialia 6 (11) (2010) 4380–4388.
[19] D.U. Tulyaganov, S. Agathopoulos, J.M.G. Ventura, M.A. Karakassides, O. Fabrichnaya, J.M.F. Ferreira, Synthesis of glass–ceramics in the CaO–MgO–SiO_2 system with B_2O_3, P_2O_5, Na_2O and CaF_2 additives, Journal of European Ceramic Society. 26 (8) (2006) 1463–1471.
[20] S. Agathopoulos, D.U. Tulyaganov, J.M.G. Ventura, S. Kannan, A. Saranti, M.A. Karakassides, J.M.F. Ferreira, Structural analysis and devitrification of glasses based on the CaO–MgO–SiO_2 system with B_2O_3, Na_2O, CaF_2 and P_2O_5 additives, Journal of Non-Crystalline Solids 352 (2006) 322–328.
[21] A. Tilocca, Structural models of bioactive glasses from molecular dynamics simulations, Proceedings of the Royal Society A 465 (2104) (2009) 1003–1027.
[22] M.L. Ernest, C.R. Robbins, H.F. Mc Murdie, Phase Diagrams for Ceramists, American Ceramic Society, Westerville OH, 2004.
[23] A.G. Tas, Synthesis of biomimetic Ca-hydroxyapatite powders at 37 °C in synthetic body fluids, Biomaterials 21 (2000) 1429–1438.
[24] L.L. Hench, Bioceramics, Journal of American Ceramic Society 81 (7) (1998) 1705–1728.
[25] V. Aina, G. Lusvardi, G. Malavasi, L. Menabue, C. Morterra, Fluoride-containing bioactive glasses: surface reactivity in simulated body fluids, Acta Biomaterialia 5 (2009) 3548–3562.
[26] L.L. Hench, J. Wilson, Surface-active biomaterials, Science 226 (4675) (1984) 630–636.
[27] I. Allan, H. Newman, M. Wilson, Antibacterial activity of particulate bioglass against supra- and subgingival bacteria, Biomaterials 22 (12) (2001) 1683–1687.
[28] P. Stoor, E. Soderling, J.I. Salonen, Antibacterial effects of a bioactive glass paste on oral microorganisms, Acta Odontologica Scandinavica 56 (3) (1998) 161–165.
[29] S. Kannan, F. Goetz-Neunhoeffer, J. Neubauer, A.H. Rebelo, P. Valério, J.M.F. Ferreira, Rietveld structure and in vitro analysis on the influence of magnesium in biphasic (hydroxyapatite and beta-tricalcium phosphate) mixtures, Journal of Biomedical Materials Research B Applied Biomaterials 90 (2009) 404–411.
[30] Y. Yamasaki, Y. Yoshida, M. Okazaki, A. Shimazu, T. Uchida, T. Kubo, Y. Akagawa, Y. Hamada, J. Takahashi, N. Matsuura, Synthesis of functionally graded $MgCO_3$ apatite accelerating osteoblast adhesion, Journal of Biomedical Materials Research 62 (1) (2002) 99–105.
[31] H. Zreiqat, C.R. Howlett, A. Zannettino, P. Evans, G. Schulze-Tanzil, C. Knabe, M. Shakibaei, Mechanisms of magnesium-stimulated adhesion of osteoblastic cells to commonly used orthopaedic implants, Journal of Biomedical Materials Research 62 (2) (2002) 175–184.
[32] E. Dietrich, H. Oudadesse, A. Lucas-Girot, Y. Le Gal, S. Jeanne, G. Cathelineau, Effects of Mg and Zn on the surface of doped melt-derived glass for biomaterials applications, Applied Surface Science 255 (2) (2008) 391–395.
[33] V. Aina, G. Malavasi, A. Fiorio Pla, L. Munaron, C. Morterra, Zinc-containing bioactive glasses: surface reactivity and behaviour towards endothelial cells, Acta Biomaterialia 5 (4) (2009) 1211–1222.
[34] D.S. Brauer, N. Karpulthina, M.D. O'Donnell, R.V. Law, R.G. Hill, Fluoride-containing bioactive glasses: effect of glass design and structure on degradation, pH and apatite formation in simulated body fluid, Acta Biomaterialia 6 (8) (2010) 3275–3282.
[35] M.A. Pogrel, Treatment of keratocysts: the case for decompression and marsupialization, Journal of Oral Maxillofacial Surgery 63 (2005) 1667–1673.
[36] H.H. Horch, R. Sader, C. Pautke, A. Neff, H. Deppe, A. Kolk, Synthetic, pure-phase beta-tricalcium phosphate ceramic granules (Cerasorb®) for bone regeneration in the reconstructive surgery of the jaws, International Journal of Oral and Maxillofacial Surgery 35 (8) (2006) 708–713.